JACS
JOURNAL OF THE AMERICAN CHEMICAL SOCIETY
Communication
pubs.acs.org/JACS

A New Nanobiocatalytic System Based on Allosteric Effect with Dramatically Enhanced Enzymatic Performance

Liang-Bing Wang,[†] You-Cheng Wang,[†,‡] Rong He,[†] Awei Zhuang,[†] Xiaoping Wang,[†] Jie Zeng,*[,†,§] and J. G. Hou[†]

[†]Hefei National Laboratory for Physical Sciences at the Microscale, [‡]School of the Gifted Young, and [§]Department of Chemical Physics, University of Science and Technology of China, Hefei, Anhui 230026, P. R. China

Supporting Information

ABSTRACT: We report a rational design of $CaHPO_4$-α-amylase hybrid nanobiocatalytic system based on allosteric effect and an explanation of the increase in catalytic activity when certain enzymes are immobilized in specific nanomaterials. Employing a calcification approach in aqueous solutions, we acquired such new nanobiocatalytic systems with three different morphologies, i.e., nanoflowers, nanoplates, and parallel hexahedrons. Through studying enzymatic performance of these systems and free α-amylase with/without Ca^{2+}, we demonstrated how two factors, allosteric regulation and morphology of the as-synthesized nanostructures, predominantly influence enzymatic activity. Benefiting from both the allosteric modulation and its hierarchical structure, $CaHPO_4$-α-amylase hybrid nanoflowers exhibited dramatically enhanced enzymatic activity. As a bonus, the new system we devised was found to enjoy higher stability and durability than free α-amylase plus Ca^{2+}.

Nanobiocatalysis, in which enzymes are immobilized in/on nanostructured materials, has attracted ever increasing attention due to its potential applications related to proteomic analysis, antifouling, biofuel cells, and tissue engineering.[1,2] In general, enzyme immobilization is hopefully expected to result in an increase in enzyme stability, which allows the industrial reuse of enzymes for more reaction cycles and thus a massive implementation of them in sustainable chemical processes. Having manifested great efficiency in manipulating the local environment of immobilized enzymes, nanomaterials, including nanoporous silica, electrospun nanofibers, magnetic nanoparticles, carbon nanotubes, and polymer beads, serve as competitive candidates in the immobilization of enzymes and many other areas of enzyme technology.[3] Thanks to the efforts from a number of research groups, nanomaterials have been employed to effectively immobilize enzymes through a number of strategies involving the "entrapment" approach and "single enzyme nanoparticles" technique.[2,4] Most of these immobilized enzymes exhibited enhanced stability compared to free enzymes in solution. Nevertheless, their activities were reduced after immobilization, which can be ascribed to three facts: (i) the use of organic solvents (i.e., hexane) during the process of immobilization, which inactivated part of the enzymes; (ii) the significant mass transfer of substrate for the immobilized enzymes; and (iii) the chemical reactions between proteins and nanomaterials during the synthesis of the nanobiocatalyst. Less frequently, there are occasions which concerns activity retaining of a majority of activity or even activity enhancement after immobilization.[3c,5] This apparently limits the possibility to apply these nanobiocatalytic systems. Recently, an encouraging breakthrough in preparation of immobilized enzymes with greatly enhanced activities was achieved by Zare and coworkers.[6] They reported the synthesis of hybrid hierarchical nanostructures comprising of copper phosphate ($Cu_3(PO_4)_2$) and enzymes via a coprecipitation method. Their success is in part built around the environment (the synthesis was conducted in an aqueous buffer solution without any organic solvent involved) and high surface area of hierarchical nanostructures. However, the mechanism exactly how activity of immobilized enzymes improved has not been amply interpreted and validated.

In biochemistry, allosteric effect denotes an interesting phenomenon that binding of a ligand to one site (which we designate as the allosteric site) on a protein molecule indirectly manipulates the properties of another specific site (the functional site and in enzymes called the active site) on the same protein as a consequence of conformational changes.[7] Some enzymes are allosteric proteins, and their activity is regulated through the binding of an effector to an allosteric site. An example of allosteric modulation is the heme−heme interaction of hemoglobin in which heme is the allosteric or active site of an adjoining protein subunit.[8] When oxygen molecules, the effectors, attach to hemes, a conformational change arises in those subunits which then interact with the remaining active sites to promote oxygen affinity. Aside from oxygen, metal ions, such as Fe^{3+}, Ca^{2+}, and Zn^{2+}, are also known to be effectors of various enzymes.[9]

Here, we aim to establish a rational design of a nanobiocatalytic system based on allosteric effect to cast light on the mechanism of how enzymatic activity increases when immobilized in nanomaterials. We selected α-amylase which is capable of hydrolyzing α-bonds of α-linked polysaccharides, such as starch and glycogen, yielding glucose and maltose to investigate this phenomenon.[10] It manifests the allosteric effect when interacted with Ca^{2+} in aqueous solutions.[11] In the absence of Ca^{2+} in an aqueous solution, most α-amylases are "inactive" with the functional sites inhibited, whereas only a few of them are "active" with the functional sites enabled. As shown

Received: December 10, 2012
Published: January 14, 2013

dx.doi.org/10.1021/ja3120136 | J. Am. Chem. Soc. 2013, 135, 1272−1275

in Figure 1A, with the involvement of Ca^{2+}, allosteric sites topographically separated from functional sites are combined

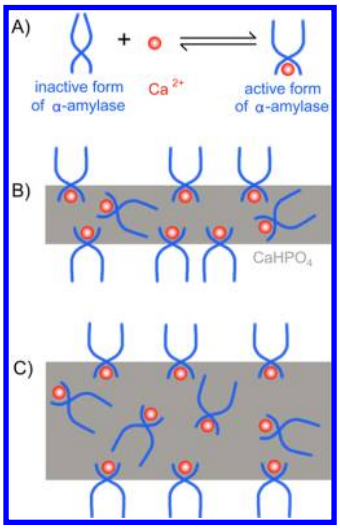

Figure 1. (A) Ca^{2+} binds to allosteric site in inactive α-amylase and generates active α-amylase. (B,C) α-amylase immobilized in thinner or thicker $CaHPO_4$ nanocrystals. The ratio of embeded α-amylase molecules to exposed ones increased with the thickness of $CaHPO_4$ nanocrystals.

with Ca^{2+} ions, thus exciting previously inactive functional sites. In other words, Ca^{2+} acts as a switch to tune the catalytic activity of α-amylase. This effect gave us the vital spark to employ a calcification process to immobilize α-amylase in calcium hydrogen phosphate ($CaHPO_4$). Owing to positive modulation of the allosteric effect induced by Ca^{2+} as effectors, the immobilized α-amylase stays in an active form. Evidently, the morphological characteristics of the nanocrystals, such as thinness, interfere with the efficiency of the nanobiocatalytic system, as illustrated in Figure 1B,C. A certain amount of α-amylases was contained in $CaHPO_4$ instead of being exposed on the surface, considerably reducing the probability of substrates to bind to active sites due to mass transfer limitation and therefore diminishing overall catalytic activity. We eventually obtained $CaHPO_4$-α-amylase hybrid nanostructures with diverse configuration, including nanoflowers, nanoplates, and parallel hexahedrons, and then examined catalytic properties of these systems along with those of free α-amylases with/without Ca^{2+} in detail. The immobilized α-amylase exhibited substantially enhanced enzymatic activity dependent on morphology. We reached a point that both the allosteric effect and morphology notably prominently influence catalytic efficiency. The nanobiocatalytic systems we devised create a feasible means of studying allosteric effects in the immobilization of enzymes.

In a standard synthesis, an aqueous solution of $CaCl_2$ (200 mM, 100 μL) was added into 5 mL of phosphate buffered saline (PBS) solution (3 mM) containing 0.2 mg/mL α-amylase at pH = 6.8. The reaction was then allowed to proceed at rt (~25 °C) for 12 h. By means of regulating the concentrations of α-amylase, PBS, and $CaCl_2$ (see SI Experimental section), we accomplished formation of nanostructures of distinctive morphology. Figure 2 shows SEM images of the products, successively demonstrating nanoflowers, nanoplates, and parallel hexahedrons. In Figures 2A and S1A, the separated nanoflowers with an average size of ~4

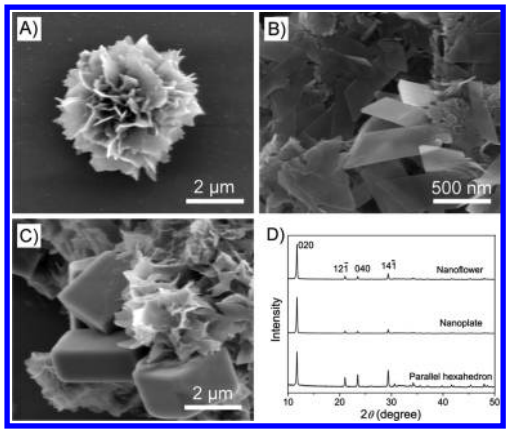

Figure 2. SEM images of (A) nanoflowers, (B) nanoplates, and (C) parallel hexahedrons. (D) XRD patterns of nanoflowers, nanoplates, and parallel hexahedrons, respectively (from top to bottom).

± 0.5 μm exhibit explicit hierarchical structure, and thickness of the petals was only in the range of 20−25 nm (Figure S1B). Further observation proved that all the petals were smooth with no pores or rifts appearing on their surfaces. Figure 2B characterized parallelogrammic nanoplates (~500 nm in width and ~30 nm in thickness) we produced with a relatively high concentration of PBS (≥15 mM). Finally, Figure 2C clearly demonstrated parallel hexahedrons mixed with fragments which were formed in the presence of a relatively high concentration of α-amylase (2 mg/mL). To corroborate the $CaHPO_4$-α-amylase hybrid structures, we implemented XRD analysis (Figure 2D). All the diffraction peaks can be indexed to the monoclinic $CaHPO_4{\cdot}2H_2O$ (JCPDS 72-0713). Furthermore, the EDX analysis (Figure S2) of nanoflowers (as an example) agreed well with the components of $CaHPO_4{\cdot}2H_2O$. We also instanced TGA of nanoflowers to shape a clearer image of the components of these systems. It is revealed that the weight percentage of organic component (i.e., α-amylase) of the untreated nanoflowers was 20.16% (Figure S3), signifying an effective hybridization of $CaHPO_4$ with α-amylase. The encapsulation efficiency (defined as the ratio of the amount of immobilized enzyme to the total amount of enzyme employed) of α-amylase in nanoflowers, nanoplates, and parallel hexahedrons was determined to be 96%, 95%, and 97%, respectively, by measuring the concentration of free α-amylase in the supernatant of the solution using the Branford protein assay[12] (see SI Experimental section).

To illuminate the impact of allosteric regulation and the morphology of nanosturctures on catalysis, we used the hydrolysis of 2-chloro-4-nitrophenylmaltotrioside (Cnp-G3) by α-amylase as a model reaction to evaluate the catalytic activities of free and immobilized α-amylase. Without catalysts, Cnp-G3 is colorless. Upon the addition of α-amylase, Cnp-G3 was gradually hydrolyzed to generate 3-chloro-4-hydroxylnitrobenzene (Chn), together with appearance of an absorbance peak at 405 nm (see eq 1).[13]

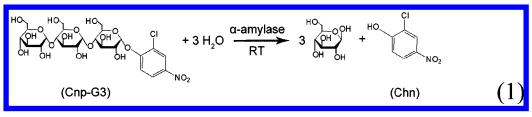

This phenomenon allows us to monitor the progress or kinetics of the reaction by colorimetric method. The absorbance (in positive correlation with the degree of reaction) of different systems at Chn peak along time is demonstrated in Figure 3A.

dx.doi.org/10.1021/ja3120136 | J. Am. Chem. Soc. 2013, 135, 1272−1275

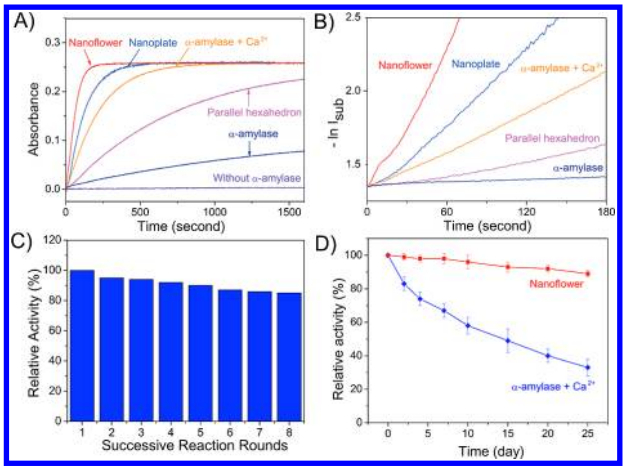

Figure 3. (A) Absorbance at the peak position for Chn (405 nm) as a function of time for six different catalytic systems. The concentration of Cnp-G3 was 0.47 mM for each system. (B) Plots of $-\ln I_{sub}$ vs time for five catalytic systems. The reaction rate constants (k) determined from these plots are 16.5×10^{-3}, 8.0×10^{-3}, 4.5×10^{-3}, 1.2×10^{-3}, and 4.4×10^{-4} s^{-1} for nanoflowers, nanoplates, free α-amylase with Ca^{2+}, parallel hexahedron, and free α-amylase, respectively. (C) Relative activity of nanoflowers over the course of eight rounds of successive reaction. (D) Storage stabilities of nanoflowers and free α-amylase in PBS (pH = 6.8) at rt.

The plot lies on the premise of setting equivalent initial concentrations of Cnp-G3 to 0.47 mM. Without the addition of free or immobilized α-amylase, no reaction was observed, affirming that hydrolysis reaction was unable to occur by itself under the experimental conditions. Upon the addition of free α-amylase (0.04 mg/mL) without Ca^{2+}, absorbance at 405 nm increased over time. Then again, adding Ca^{2+} (20 μL of 100 mM $CaCl_2$ solution) to free α-amylase (0.04 mg/mL) brought about an even higher absorbance. In $CaHPO_4$-α-amylase systems (the concentrations of α-amylase put in were all 0.04 mg/mL), absorption enhanced significantly. Among them, the catalytic reaction rate of nanoflowers ranked the first, nanoplates the second, and parallel hexahedrons the last. Compared to free α-amylase, nanoflowers and nanoplates displayed stronger while parallel hexahedrons weaker absorbance.

Note that in the reaction system, the concentration of H_2O greatly exceeded that of Cnp-G3, so it is not unreasonable to consider its concentration as a constant during the reaction. The pseudofirst-order kinetics with respect to Cnp-G3 could be applied to our experimental system. The approximately linear shape of the plot of $-\ln I_{sub}$ (I_{sub} is the value obtained by subtracting the real-time absorbance from the saturated one, i.e., 0.26) vs time, as shown in Figure 3B, supports the pseudofirst-order assumption. Based on the linear relationship, the average reaction rate constants (k) were calculated to be 4.4×10^{-4}, 4.5×10^{-3}, 16.5×10^{-3}, 8.0×10^{-3}, and 1.2×10^{-3} s^{-1} when the free α-amylase without Ca^{2+} /with Ca^{2+} and those after incorporation in nanoflowers, parallelogrammic plates, and parallel hexahedrons were employed as the catalysts, respectively. To support, we calculated Michaelis constant (K_m) of each system (data shown in Figure S4).[14] It was found that nanoflowers undertook the lowest K_m value, confirming that they have a higher efficiency to convert Cnp-G3 into products. All tests concerning catalysis were performed after concentrations of α-amylase (whether immobilized or not) in all systems were adjusted to be identical.

All the facts and statistics above proved that Ca^{2+} favors catalytic activity, which can be accredited to allosteric regulation, as mentioned beforehand. It is also confirmed that immobilization of α-amylase in $CaHPO_4$ strongly associates with catalytic activity. In fact, when concentrations of α-amylase were kept the same, two factors, the action of Ca^{2+} (or the allosteric effect it induces) and morphology of the structures, dominate the system, as they constitute variables in our experimental design. First, because α-amylase, like a variety of proteins or enzymes, is endowed with the ability of allosteric interaction, both addition of Ca^{2+} into free α-amylase and immobilization of α-amylase in $CaHPO_4$ nanocrystals lead to allosteric effect where Ca^{2+} functions as effectors and bind to specific functional sites. After this combination, α-amylase experiences conformational changes and remains in the "active form". Conceivably, immobilization is seized at a higher conversion of the inactive α-amylase to active α-amylase than addition of Ca^{2+} directly into free α-amylase. On the basis of a same total amount of enzyme, immobilization seems to hold more α-amylase in "active form". For that reason, the three systems, nanoflowers, nanoplates, and parallel hexahedrons, are primarily supposed to earn a more preferable activity than free α-amylase with Ca^{2+} (although parallel hexahedrons make an exception). Second, morphology is also an important factor that contributes to the differences in activity. Nanoflowers and nanoplates obviously enjoyed higher surface-to-volume ratio than parallel hexahedrons as a result of less significant mass transfer limitations. In consequence, a larger portion of immobilized α-amylase rests on the surface (Figure 1B,C), having a bigger possibility to meet the substrate molecules. On the contrary, parallel hexahedrons conceal a great part of immobilized α-amylase and eventually prevent them from acting as enzymes. In our experiment, the compensation paid by immobilization even fails to cover the hiding of α-amylase.

The reason why nanoflowers exceed nanoplates in activity lies in that although nanoplates approximates petals of the nanoflowers in thinness, they have a greater likelihood to self-assemble, which is disastrous to activity. When they overlap, nanoplates virtually lower the ratio of immobilized α-amylase on the surface. However, nanoflowers consist of many dispersive petals that expel rather than connect to each other (Figure S1). They hold higher catalytic activity at a lower cost of enveloping α-amylase inside the nanostructure. These inspiring results indicate characteristic properties of nano-biocatalytic systems with high catalytic activity: large surface-to-volume ratio and hierarchical or isolated structure without assembling.

The attractive catalytic activity of $CaHPO_4$-α-amylase hybrid nanoflowers makes it plausible to use them as a nanobiocatalyst. To substantiate this, their stability and durability were tested. Figure 3C shows the plot of relative activity against the number of successive catalytic reactions that repeatedly used the α-amylase-incorporated nanoflowers as the catalyst. It is clear that the nanoflowers only lost 16% of their catalytic activity over the course of eight rounds of reaction, demonstrating a high durability. As for the stability test (Figure 3D), the free enzyme (adding Ca^{2+} when tested) lost 67% of its initial activity within 25 days when incubated in PBS (pH = 6.8) at rt, whereas under the same condition, nanoflowers maintained most of their initial activity (~90%). It is worth pointing out that all the tests did not result in any obvious morphological change for the nanoflowers (Figure S5), indicating that the nanoflowers were highly stable in the chemical environment of the catalytic

dx.doi.org/10.1021/ja3120136 | J. Am. Chem. Soc. 2013, 135, 1272−1275

reaction although they have a large surface area and thereby a high surface energy.

In conclusion, to investigate the previously observed phenomenon that certain enzymes exhibited increased activity after immobilized in specific nanomaterials and to verify the impact of allosteric regulation, we designed a series of novel nanobiocatlytic systems, i.e., nanoflowers, nanoplates, and parallel hexahedrons, the enzymatic activities of which were compared with those of free α-amylase with/without Ca^{2+}. We interpreted the phenomenon as an end product of mainly two factors: allosteric effect of Ca^{2+} ions with the amine groups of α-amylase and morphology of nanostructures. Among these systems, the hierarchically structured hybrid nanoflowers exhibited the best enzymatic performance. Our design also provides a convenient and environmentally benign route to large-scale production because the process does not involve high temperature or organic solvents. Plus with the biocompatibility of $CaHPO_4$ and the high stability and durability, this new biocatalytic system based on allosteric effects is promising to find widespread use in applications related to biomedicine, biofuel cells, biosensor, and tissue engineering.

■ ASSOCIATED CONTENT

Supporting Information

Experimental details, SEM images, EDX spectrum, and TGA data. This material is available free of charge via the Internet at http://pubs.acs.org.

■ AUTHOR INFORMATION

Corresponding Author

zengj@ustc.edu.cn

Notes

The authors declare no competing financial interest.

■ ACKNOWLEDGMENTS

This work was supported by MOST of China (2011CB921403), NSFC under grant nos. 21203173 and 21121003, 51132007 and J1030412, and CAS. J.Z. also thanks the University of Science and Technology of China for the startup funds.

■ REFERENCES

(1) (a) Luckarift, H. R.; Spain, J. C.; Naik, R. R.; Stone, M. O. *Nat. Biotechnol.* **2004**, *22*, 211. (b) Chiu, C. Y.; Li, Y.; Ruan, L.; Ye, X.; Murray, C. B.; Huang, Y. *Nat. Chem.* **2011**, *3*, 393. (c) Kim, J.; Grate, J. W.; Wang, P. *Trends Biotechnol.* **2008**, *26*, 639. (d) Ge, J.; Lu, D.; Liu, Z.; Liu, Z. *Biochem. Eng. J.* **2009**, *44*, 53. (e) Zeng, J.; Xia, Y. *Nat. Nanotechnol.* **2012**, *7*, 415. (f) Mann, S. *Nat. Mater.* **2009**, *8*, 781.

(2) (a) Kim, J.; Grate, J. W. *Nano Lett.* **2003**, *3*, 1219. (b) Yan, M.; Ge, J.; Liu, Z.; Ouyang, P. *J. Am. Chem. Soc.* **2006**, *128*, 11008.

(3) (a) Lee, C. H.; Lin, T. S.; Mou, C. Y. *Nano Today* **2009**, *4*, 165. (b) Cao, A.; Ye, Z.; Cai, Z.; Dong, E.; Yang, X.; Liu, G.; Deng, X.; Wang, Y.; Yang, S. T.; Wang, H.; Wu, M.; Liu, Y. *Angew. Chem., Int. Ed.* **2010**, *49*, 3022. (c) Lei, C.; Shin, Y.; Liu, J.; Ackerman, E. J. *J. Am. Chem. Soc.* **2002**, *124*, 11242. (d) Xin, B.; Xing, G. *Prog. Chem.* **2010**, *22*, 593. (e) Kim, J.; Grate, J. W.; Wang, P. *Chem. Eng. Sci.* **2006**, *61*, 1017.

(4) (a) Daubresse, C.; Grandfils, C.; Jerome, R.; Teyssie, P. *J. Colloid Interface Sci.* **1994**, *168*, 222. (b) Ma, D.; Li, M.; Patil, A. J.; Mann, S. *Adv. Mater.* **2004**, *16*, 1838. (c) Kim, J.; Kim, B. C.; Lopez-Ferrer, D.; Petritis, K.; Smith, R. D. *Proteomics* **2010**, *10*, 687.

(5) (a) Dulay, M. T.; Baca, Q. J.; Zare, R. N. *Anal. Chem.* **2005**, *77*, 4604. (b) Sui, X. H.; Lin, T. Y.; Tleugabulova, D.; Chen, Y.; Brook, M. A.; Brennan, J. D. *Chem. Mater.* **2006**, *18*, 887. (c) Livage, J.; Coradin, T.; Roux, C. *J. Phys.: Condens. Matter* **2001**, *13*, R673. (d) Frenkel-Mullerad, H.; Avnir, D. *J. Am. Chem. Soc.* **2005**, *127*, 8077.

(6) Ge, J.; Lei, J.; Zare, R. N. *Nat. Nanotechnol.* **2012**, *7*, 428.

(7) (a) Sijbesma, R. P.; Nolte, R. J. M. *J. Am. Chem. Soc.* **1991**, *113*, 6695. (b) Monod, J.; Wyman, J.; Changeux, J. P. *J. Mol. Biol.* **1965**, *12*, 88.

(8) Edelstein, S. J. *Annu. Rev. Biochem.* **1975**, *44*, 209.

(9) (a) Libman, J.; Tor, Y.; Shanzer, A. *J. Am. Chem. Soc.* **1987**, *109*, 5880. (b) Zhang, X.; Solaro, C. R.; Lingle, C. J. *J. Gen. Physiol.* **2001**, *118*, 607. (c) Swaminath, G.; Steenhuis, J.; Kobilka, B.; Lee, T. W. *Mol. Pharmacol.* **2002**, *61*, 65.

(10) Uitdehaag, J. C. M.; Mosi, R.; Kalk, K. H.; van der Veen, B. A.; Dijkhuizen, L.; Withers, S. G.; Dijkstra, B. W. *Nat. Struct. Biol.* **1999**, *6*, 432.

(11) (a) Vihinen, M.; Mantsala, P. *Crit. Rev. Biochem. Mol.* **1989**, *24*, 329. (b) Machius, M.; Wiegand, G.; Huber, R. *J. Mol. Biol.* **1995**, *246*, 545. (c) Vallee, B. L.; Stein, E. A.; Sumerwell, W. N.; Fischer, E. H. *J. Biol. Chem.* **1959**, *234*, 2901. (d) Violet, M.; Meunier, J. C. *Biochem. J.* **1989**, *263*, 665.

(12) (a) Pollard, H. B.; Menard, R.; Brandt, H. A.; Pazoles, C. J.; Creutz, C. E.; Ramu, A. *Anal. Biochem.* **1978**, *86*, 761. (b) Compton, S. J.; Jones, C. G. *Anal. Biochem.* **1985**, *151*, 369.

(13) Haupt, B.; Neumann, T.; Wittemann, A.; Ballauff, M. *Biomacromolecules* **2005**, *6*, 948.

(14) Dowd, J. E.; Riggs, D. S. *J. Biol. Chem.* **1965**, *240*, 863.